Supplementary Material

For the manuscript "High-income does not protect against hurricane losses"

Tobias Geiger[1,*], Katja Frieler[1], Anders Levermann[1,2,3]

[1]Potsdam Institute for Climate Impact Research,

Telegraphenberg A56, D - 14473 Potsdam, Germany.

[2]LDEO, Columbia University,

61 Route 9w, Palisades, NY 10964, USA.

[3]Institute of Physics, Potsdam University,

Karl-Liebknecht-Str. 24/25, D - 14476 Potsdam, Germany.

* corresponding author: geiger@pik-potsdam.de

This supplementary material provides details of data preparation and data analysis but also includes additional results referred to in the main text. It provides future loss projections for all SSP-scenarios and details about the underlying contribution from each GCM, each damage function and each loss data set.

Preparation of hurricane tracks

Historic hurricane wind-field extensions are reconstructed based on NOAA's HURDAT2 best track archive[1] (extended version) using 6h track coordinates, maximum wind-speed (V_{max}), and wind-speed radii for the wind-speed thresholds 64knts and V_{max}. The track coordinates are linearly interpolated to hourly data. For each coordinate the local wind-field extension of 64knts and V_{max} is based on the mean radii information reported in the HURDAT2 archive and transferred to a grid with spatial resolution of 0.1° x 0.1° (approx. 10 km x 10 km). Where wind-speed radii are unavailable (prior to 1988 and missing data), the wind-field is a best estimate based on the full record from 1988-2012. Table S1 shows wind-field radii depending on V_{max} used for reconstruction. The temporally-aggregated wind-field for each

hurricane is obtained by taking the maximum of all wind-field values for each track coordinate. Figure S1 illustrates the wind-field for hurricane Katrina (2005) and hurricane Betsy (1965). Whereas Katrina's wind-field is reconstructed from empiric data, Betsy's wind-field is estimated according to Table S1. We additionally verified that using wind-field estimates based on a parametric wind-field model[2] yields similar fit parameters as reported in our analysis. Simulated hurricane tracks for the historic (1950-2005) and future climate under RCP8.5 (2006-2100) are obtained from Kerry Emanuel[3], see the original publication for details. Simulated tracks are equivalently interpolated to hourly data, each storm's wind-field is estimated using the 1988-2012 wind radii record, and projected to a grid with 0.1° resolution. For all tracks (empiric and simulated) the range of 64 knts winds is used to define the affected capital stock assuming that 1-min sustained winds below 64 knts create negligible damage. We thereby introduce a physical measure for affected capital stock per grid cell rather than relying on more coarse and possibly subjective estimates of affected (coastal) counties or larger administrative regions. (Nonetheless, we obtain very similar fit results when repeating our analysis for affected coastal counties only, c.f. Table S6 and Table S7.) In order to ensure consistency between empiric and simulated tracks, the wind-speed at landfall is obtained from our own wind-field estimates as the maximum V_{max} value recorded over land. We only detect minor differences with respect to the HURDAT2-reported wind-speed at landfall (the wind-speed at landfall is not provided for all hurricanes of interest). This assumption led to the inclusion of Superstorm Sandy (2012) as a hurricane into our analysis as our wind-field estimates indicate sustained winds above 64 knts on land.

Hurricane loss data

Hurricane losses are often difficult to value and are based on reported (insured) losses by various agencies, additional estimates, as well as guess-work, c.f. Ref. 4. In order to verify the robustness of our results, two different loss data sets are included in our analysis. The ICAT loss data base (www.icatdamageestimator.com) recollects the losses reported by the National Hurricane Center. The available time-series extends back to 1900 (we analyze 1963-2012) but loss estimates are reported as is without further re-analysis. On the contrary, the proprietary NATCAT data base by MunichRE's NATCATSERVICE[5] is maintained and constantly updated, with the drawback that the record extends only back to 1980. For reasons of model-

comparability, we use full (i.e. insured + uninsured) historic losses. In both data sets losses are reported in values corresponding to the year of landfall, which we subsequently inflation-adjust to 2005$ based U.S. consumer price time series (www.bea.gov).

It is well known that loss data reporting and accuracy has significantly improved over time. We find signatures of changing data quality also in our analysis. The explained variances for damage models based on ICAT and NATCAT data is very similar when analyzed for identical time periods (see Table S10 and Table S11) but diverges when ICAT is analyzed from 1963-2012 instead of 1980-2012 (see Table S4 and Table S5). Because of statistical (more hurricane counts) and robustness (different time periods) reasons the results presented in the main text rely on ICAT data for the period 1963-2012.

Socio-economic predictors

All socio-economic variables are prepared on a grid with 0.1° resolution, in accordance with the track data. We require socio-economic variables that best reflect the local distribution of assets and for which future projections are readily available. Therefore, per capita GDP and population is chosen instead of capital stock data. When analyzed over time, we observe a good proportionality between national GDP and the 'fixed assets and durable goods' time series (provided by www.bea.gov) making GDP a valid proxy for capital stock, c.f. also Refs. 6,7. We assume that the underlying grid resolution of 0.1° is small enough to detect local differences in population and income but also large enough not to violate the validity of GDP as a proxy. Differences in GDP across U.S. States are preserved by using U.S. States GDP time series (inflation-adjusted to $2005) that are available from www.bea.gov back to 1963. Based on State population data (from www.census.gov) per capita GDP is determined and distributed according to a high-resolution gridded population density time series using 2000 high-resolution (0.0083°) Gridded Population of the World (GWPv3) data[8] normalized according to US county population and county population changes[9]. Projected future population density according to five different SSP scenarios[10] is downscaled from its original 0.125° resolution to match our grid resolution.

Future GDP estimates are based on national per capita GDP evolution according to

different SSPs (https://tntcat.iiasa.ac.at/SspDb) and gridded future population time series. In order to conserve local inhomogeneities in per capita GDP distribution, national per capita GDP is rescaled according to the historic mean (2008-2012) of US States GDP per capita.

Damage model derivation based on empiric data

The damage models that use GDP as a single predictor for socio-economic development (basic model type 1) are summarized in Table S2. We obtain eight loss estimates by combining the input of the two different loss data sets and four distinct functional forms:

$$\log(Loss_j) = \alpha + \beta_{GDP} \times \log(GDP_j) + \gamma \times \log(V_{max,j}) + \varepsilon_j, \quad (1)$$

$$\log(Loss_j) = \alpha + \beta_{GDP} \times \log(GDP_j) + \gamma \times V_{max,j} + \varepsilon_j, \quad (2)$$

$$\log(Loss_j) = \alpha + \log\left[\sum_i^{j_v}\left[(GDP_{ij})^{\beta_{GDP}} \times (V_{max,ij})^{\gamma}\right]\right] + \varepsilon_j, \quad (3)$$

$$\log(Loss_j) = \alpha + \log\left[\sum_i^{j_v}\left[(GDP_{ij})^{\beta_{GDP}} \times exp(\gamma \times V_{max,ij})\right]\right] + \varepsilon_j. \quad (4)$$

Damage functions (1) – (4) are called sub-type 1 – 4 (sub-type 5 – 8) in Table S2 if derived using ICAT (NATCAT) loss data base.
The damage functions in Table S3 separate the socio-economic predictors population and per capita GDP (basic model type 2):

$$\log(Loss_j) = \alpha + \beta_{Pop} \times \log(POP_j) + \beta_{GDPpc} \times \log(GDPpc_j) + \gamma \times \log(V_{max,j}) + \varepsilon_j, \quad (5)$$

$$\log(Loss_j) = \alpha + \beta_{Pop} \times \log(POP_j) + \beta_{GDPpc} \times \log(GDPpc_j) + \gamma \times V_{max,j} + \varepsilon_j, \quad (6)$$

$$\log(Loss_j) = \alpha + \log\left[\sum_i^{j_v}\left[(Pop_{ij})^{\beta_{Pop}} \times (GDPpc_{ij})^{\beta_{GDPpc}} \times (V_{max,ij})^{\gamma}\right]\right] + \varepsilon_j, \quad (7)$$

$$\log(Loss_j) = \alpha + \log\left[\sum_i^{j_v}\left[(Pop_{ij})^{\beta_{Pop}} \times (GDPpc_{ij})^{\beta_{GDPpc}} \times exp(\gamma \times V_{max,ij})\right]\right] + \varepsilon_j \quad (8)$$

Damage functions (5) – (8) are called sub-type 1 – 4 (sub-type 5 – 8) in Table S3 if derived using ICAT (NATCAT) loss data base.
A (non-linear) least-square Levenberg-Marquardt algorithm is used to determine the fit parameters ($\alpha, \beta_{Pop}, \beta_{GDP}, \beta_{GDPpc}, \gamma$), their corresponding standard errors, and the adjusted R^2-values for all damage functions of sub-type 1 – 8 for both basic model

versions, see Table S4 and Table S5. We verified that the residuals ε_j of Eqs. (1) – (8) are normally distributed such that the standard errors provide good measures of uncertainty. The R^2-values provided for models of sub-type 3, sub-type 4, sub-type 7, and sub-type 8 result from non-linear regression for which a properly defined R^2-value (that is bounded between [0,1]) does not necessarily exist. However, the correctness of the given R^2-values is verified by the fact that the square of the Pearson correlation in Table S2 and Table S3 corresponds to the R^2-values reported in Table S4 and Table S5, both, for linear (function type: global) and non-linear (function type: local) regression results.

The number of hurricanes in our regression analysis is limited due to data-availability and data-quality: the loss data set by Munich Re was only initiated in 1980 while U.S. States GDP data was collected only from 1963 onwards. Nonetheless do we find highly significant regression results for most of our loss estimates, c.f. Table S4 and Table S5. Using total GDP as a predictor of socio-economic development (Table S4), we find a significant sub-linear scaling of losses with affected GDP across all models. The model prefactor α is, however, non-significant for three of the models that explore an exponential relationship between wind-speed and losses. We nonetheless use the predictions by all models in our analysis as our focus lies on average losses only and the variability of projected losses caused by different functional representations of the physical hazard is minor to the loss variability obtained by the separation of the socio-economic predictors, see Figure S9.
If the socio-economic predictors population and income are separated (Table S5), losses scale super-linearly with affected income and sub-linearly with population across all models. The statistical-significant non-linear scaling of hurricane losses with different socio-economic predictors is displayed in Figure 3 in the main text (for the damage function of sub-type 1) and in Figure S4 (sub-type 2), Figure S5 (sub-type 5), and Figure S6 (sub-type 6). The non-linear scaling for damage functions using local wind-speed estimates (sub-types 3,4,7, and 8) cannot be represented visually using the same methodology and we refer to the fit results in Table S4 and Table S5 instead. For two of those models (sub-type 3 and sub-type 4 in Table S5) the parameter β_{GDPpc}, albeit being larger than 1, does not differ significantly from unity, i.e. we cannot reject the possibility that in this particular case losses scale linearly with income. Table S5 also illustrates the different outcome for the two loss

data sets (ICAT: sub-type 1-4; NATCAT: sub-type 5-8): The effect of super-linear scaling of losses with income is somewhat smaller for ICAT than for NATCAT possibly illustrating a more recent increase in vulnerability (since 1980). This finding is supported by Table S11 where we find a very similar super-linear scaling for ICAT data analyzed for the same period as NATCAT data.

The super-linear scaling of losses with per capita GDP is contrasted by a sub-linear scaling with population. This opposing effect of both socio-economic drivers leads to a highly-nonlinear scaling and non-significant fit results for β_{Pop} for sub-type 7 and sub-type 8 in Table S5. While the cause of this highly non-linear behavior is so far elusive (ICAT-related fit parameters are somewhat comparably low for sub-type 3 and sub-type 4 in Table S5 and Table S11), we verified that omission of model sub-types 7 and 8 does not alter the main findings of this paper.

Table S4 and Table S5 also give an overview over the different power-law exponents, c.f. sub- type 1, sub-type 3, sub-type 5, and sub-type 7. Depending on the specific damage function, we find that the exponent of the non-linear damage wind-speed relationship can take values as low as 4 (close to the cubed relationship favored by ref. 11) and larger than 7 (close to the cases of 8 and 9 observed by ref. 12). Their specific choice is strongly model- as well as loss data-dependent and the search for a specific standard value may be misleading and of low relevance as the representations of the physical hazard as captured by the individual sub-models contributes less to the variability of projected future losses than the separation of the socio-economic predictors (see Figure S9).

As mentioned in the main text, Figure 2 compares the predictive quality of all eight damage estimates used in our study, analyzed for both basic model versions that either use total GDP (Figure 2a) or separate total GDP into per capita GDP and population (Figure 2b). The explained variances are high across all damage functions. The differences in explained variances for damage models based on ICAT and NATCAT data (see Table S4 and Table S5) vanishes if both loss data sets are analyzed for identical time periods (see Table S10 and Table S11).

Damage functions of different basic model type but identical sub-type reproduce historic losses almost equally well, see the Pearson correlation in Table S2 and Table S3. All damage function sub-types with separated socio-economic predictors, however, slightly outperform the corresponding sub-type based on total GDP. This increase in predictive quality is not due to the inclusion of an additional parameter as

confirmed by the Akaike Information Criterion (AICc) (with correction for small sample size)[13]. The AICc must be compared for identical damage function sub-types between Table S2 and Table S3 only; absolute AICc values across different damage function sub-types are incomparable due to different underlying data sets and functional forms.
As a robustness check, all fit parameters are again determined using affected coastal counties instead of the affected area as prescribed by the extension of hurricane-power winds, see Table S6 and Table S7. The very similar parameter dependence across all damage models underlines the independence of our finding from a change in affected population and average affected income and supports the significance of a super-linear scaling between income and losses.

Future loss projections

In addition to the results presented in the main text, we here quantify future loss projections for all five different socio-economic development scenarios and different percentiles of the loss distribution. Additionally, the impact of different GCMs, different loss data sets, and different functional representations of the physical hazard on future loss variability is analyzed.
As mentioned in the main text, the losses obtained for simulated hurricane events are normalized in order to achieve consistent projections across different GCMs and for comparability reasons with respect to historical observations. Depending on the GCM, the number of simulated tracks exceeds observations by a factor of eight. This large number of available tracks effectively samples many centuries worth of hurricane impacts along the full coastline. Hurricane losses for each GCM are normalized such that the median of empiric and simulated losses for the period 1983-2012 is equal. This intensity normalization ensures that simulated losses per event are on average identical to observed losses and that absolute loss values can be reported. Intensity normalization is conducted routinely for all simulated data. See Figure S2 for an overview of the normalization factors used to calibrate intensities. Frequency normalization is only conducted for data used in Figure 6 and Figure 7 (in the main text) and Figure S12, where loss counts above threshold and annual losses are reported, respectively. Simulated hurricane frequency is normalized such that the mean number (1993-2012) of land-falling hurricanes is equal in both, observations

and simulations. See Figure S3 for an overview of the normalization factors used to calibrate landfall frequencies. We verified that the choice of a different time interval of 30 years (1983-2012) does not change our findings as the mean frequency is very similar. Longer intervals, however, seem not adequate as they cover potentially existing trends in hurricane frequency, whereas shorter intervals are subject to fluctuations caused by natural variability.

Figure S7 and Figure S8 respectively present median and 95% percentile losses for all SSPs (SSP1-SSP5) in addition to Figure 6 presented in the main text. The SSP-specific growth trajectories for population and income in combination with the non-linear scaling of socio-economic predictors leads to diverging loss trajectories across different SSPs, even though losses are normalized relative to their scenario-specific GDP. Scenarios that assume a rapid income rise (SSP4, SSP5) see median (95% percentile) losses per storm rise by more than 300% (500%) by the end of this century with single 95% percentile events destroying regularly more than 1% of the nation's GDP. The overall tendency, however, is similar across all SSPs: Increasing income is projected to drive hurricane losses and particularly high-percentile losses will increase over-proportionally. Due to the non-linear socio-economic enhancement a few major storms (especially towards the end of this century) project higher losses than the value of actually affected GDP. The maximum loss per storm is therefore limited to the value of the affected capital stock (defined as three-times the affected GDP). Being aware that the SSP2 scenario (and all other SSPs except SSP5) might not be compatible with global warming trends under RCP8.5, we nonetheless display all scenarios in order to illustrate that the most important contribution to projected future losses is socio-economically-driven and occurs across all SSPs. A more realistic treatment would require a different hurricane climatology for each RCP, that, however, would not fundamentally change the present finding as the contribution of climate change on future losses is not the dominant driver and the inter-GCM variability is large, c.f. Figure 5 in the main text and Figure S11.

As referred to in the main text, the spread in projected losses caused by the separation of socio-economic predictors contributes more than the variability caused by the different functional representations of the physical hazard as captured by the individual sub-models (see Figure S9) and more than the variability caused by different loss data sets if both loss data sets are analyzed for identical time periods

(see Figure S10). The spread in projected losses as caused by the individual sub-models is largely caused by their different integration of wind-field data. Damage functions that rely on maximum wind-speed at landfall only (sub-types 1, 2, 5, and 6 in Table S4 and Table S5 and dashed lines in Figure S9) project higher losses than damage functions that respect the local distribution of maximum winds (sub-types 3, 4, 7, and 8 in Table S4 and Table S5 and dotted lines in Figure S9). Similarly, losses projected based on NATCAT data are always larger than losses predicted based on ICAT data (see Figure S10). The difference is especially large when population and per capita GDP are treated as separated predictors (blue shaded plus hatched region in Figure S10) but to which, however, the different analyzed time periods for each loss data set contribute mostly. When analyzed for identical periods (red-shaded area in Figure S10), the reduction in variability simultaneously results in an additional increase of average projected future losses (red solid line) due to a stronger super-linear scaling of losses with per capita income that is consistently found for both loss models for the period since 1980, see Table S5 and Table S11.

The findings up to Figure S10 are projections based on the median over all 6 GCMs. In Figure S11 each GCM is analyzed separately for the development scenario SSP2. The loss trajectory for each GCM is more volatile as projections are based on fewer events and GCM-specific variations in time become visible. All GCMs project rising loss trends towards the end of this century but with varying magnitude. With respect to 2010 values, MPI-ESM-MR projects a doubling of losses while MIROC5 sees an increase by 600%. By taking the median over all GCMs for all loss projections extreme outliers are discarded.

In contrast to per hurricane losses, annual losses are cumulated losses that can change due to changes in hurricane intensity and frequency. As illustrated in Ref. 3, intensity as well as frequency increases are expected for the North Atlantic. Consequently, both effects trigger annual loss rises, depicted as median loss changes for all SSPs in Figure S12. Under SSP2, annual losses are projected to rise by almost 750% towards the end of this century, while the fast-development scenarios (SSP4, SSP5) even estimate losses to rise by almost 1300%. We note that the scientific agreement on future hurricane intensity changes is higher than on future frequency changes[3,14–18]. Nonetheless, there exists supporting evidence that

dynamical downscaling techniques are capable of reliably reproducing observed intensity and frequency distributions[19,20].

Table S1: Local wind-field extension regressed from observed local maximum hurricane wind-speed. Values are obtained as a best-fit result based on all hurricanes for which wind-radii are available in the HURDAT-archive, see text for details.

	64 knts ≤ V_{max} < 83 knts	**V_{max} ≥ 83 knts**
Radius of 64 knts winds	0.6°	0.8°
Radius of V_{max}	0.5°	0.4°

Table S2: Detailed overview of damage function types with socio-economic scaling proportional to GDP (basic model type 1). The 8 damage functions differ with respect to their loss data and time period (ICAT/NATCAT), to their general form (global/local), and their functional wind-speed dependence (power-law/exponential). Pearson's correlation between empiric and modeled losses is obtained according to **Figure S5**a. The AICc is the Akaike Information Criterion with correction for small sample size.

damage func.	socio-eco. scaling	loss data	# hurricanes	func. type	vmax-scaling	Pearson's r	AICc
type 1-1	GDP	icat-1963	81	global	power	0.78	160.6
type 1-2	GDP	icat-1963	81	global	exp	0.78	162.6
type 1-3	GDP	icat-1963	81	local	power	0.74	175.4
type 1-4	GDP	icat-1963	81	local	exp	0.74	175.0
type 1-5	GDP	natcat-1980	53	global	power	0.83	105.7
type 1-6	GDP	natcat-1980	53	global	exp	0.82	106.3
type 1-7	GDP	natcat-1980	53	local	power	0.81	108.8
type 1-8	GDP	natcat-1980	53	local	exp	0.81	108.8

Table S3: Detailed overview of damage function types with socio-economic scaling proportional to population and per capita GDP (basic model type 2). Same as **Table S2** except for the socio-economic scaling. Pearson's correlation between empiric and modeled losses is obtained according to **Figure S5**b.

damage func.	socio-eco. scaling	loss data	# hurricanes	func. type	vmax-scaling	Pearson's r	AICc
type 2-1	Pop/GDPpc	icat-1963	81	global	power	0.80	157.1
type 2-2	Pop/GDPpc	icat-1963	81	global	exp	0.79	159.0
type 2-3	Pop/GDPpc	icat-1963	81	local	power	0.75	174.2
type 2-4	Pop/GDPpc	icat-1963	81	local	exp	0.76	173.4
type 2-5	Pop/GDPpc	natcat-1980	53	global	power	0.84	103.8
type 2-6	Pop/GDPpc	natcat-1980	53	global	exp	0.84	104.0
type 2-7	Pop/GDPpc	natcat-1980	53	local	power	0.83	106.3
type 2-8	Pop/GDPpc	natcat-1980	53	local	exp	0.84	105.5

Table S4: Fit parameters for all damage functions with socio-economic scaling proportional to GDP (basic model type 1). Fit parameters and standard errors based on (non-linear) least square fitting procedure. The damage function sub-types are summarized in **Table S2**, the goodness of fit is indicated by the corresponding R^2-value in the last column. Values marked with a * differ non-significantly from zero.

damage func.	α	$\Delta\alpha$	β_{GDP}	$\Delta\beta_{GDP}$	γ	$\Delta\gamma$	R^2
type 1-1	5.55e-07	1.34e-07	0.64	0.08	4.36	0.78	0.61
type 1-2	2.09*	5.53	0.65	0.09	0.044	0.008	0.60
type 1-3	1.33e-07	4.47e-08	0.50	0.15	5.17	1.11	0.54
type 1-4	9.18*	12.24	0.49	0.15	0.057	0.012	0.54
type 1-5	5.02e-09	1.21e-09	0.65	0.10	5.39	1.12	0.68
type 1-6	0.60*	2.59	0.67	0.10	0.057	0.012	0.68
type 1-7	3.17e-08	1.08e-08	0.20	0.18	6.86	1.32	0.66
type 1-8	719.77	357.84	0.21	0.18	0.075	0.015	0.66

Table S5: Fit parameters for all damage functions with socio-economic scaling proportional to population and per capita GDP (basic model type 2). Fit parameters and standard errors based on (non-linear) least square fitting procedure. The damage function sub-types are summarized in **Table S3**, the goodness of fit is indicated by the corresponding $\boldsymbol{R^2}$-value in the last column. Values marked with a * (+) differ non-significantly from zero (unity).

damage func.	$\boldsymbol{\alpha}$	$\Delta\boldsymbol{\alpha}$	$\boldsymbol{\beta_{Pop}}$	$\Delta\boldsymbol{\beta_{Pop}}$	$\boldsymbol{\beta_{GDPpc}}$	$\Delta\boldsymbol{\beta_{GDPpc}}$	$\boldsymbol{\gamma}$	$\Delta\boldsymbol{\gamma}$	$\boldsymbol{R^2}$
type 2-1	1.17e-12	2.74e-13	0.56	0.09	1.77	0.48	4.91	0.79	0.64
type 2-2	2.27e-05	1.08e-05	0.58	0.09	1.82	0.49	0.050	0.008	0.63
type 2-3	8.32e-13	2.39e-13	0.37	0.17	1.48+	0.55	5.84	1.09	0.56
type 2-4	3.91e-04	2.85e-04	0.36	0.17	1.52+	0.55	0.065	0.012	0.56
type 2-5	8.93e-20	2.62e-20	0.57	0.11	3.00	1.15	5.71	1.10	0.71
type 2-6	9.81e-12	4.57e-12	0.59	0.11	3.13	1.15	0.061	0.012	0.71
type 2-7	8.44e-20	2.46e-20	0.13*	0.17	2.70	1.11	7.11	1.25	0.69
type 2-8	5.69e-10	3.12e-10	0.12*	0.17	2.90	1.11	0.079	0.014	0.70

Table S6: Fit parameters for all damage functions for basic model type 1 and restricted to coastal counties. Same as **Table S4** but the affected GDP is limited to the coastal counties affected by hurricane-power winds.

damage func.	α	$\Delta\alpha$	β_{GDP}	$\Delta\beta_{GDP}$	γ	$\Delta\gamma$	R^2
type 1-1	1.49e-07	3.38e-08	0.62	0.08	4.81	0.77	0.60
type 1-2	3.03*	5.42	0.63	0.09	0.048	0.008	0.59
type 1-3	2.33e-08	6.25e-09	0.45	0.14	5.85	0.97	0.54
type 1-4	16.37	15.46	0.45	0.14	0.063	0.011	0.53
type 1-5	1.73e-09	4.14e-10	0.60	0.10	5.96	1.14	0.65
type 1-6	1.68*	7.53	0.62	0.10	0.063	0.013	0.65
type 1-7	3.92e-09	1.10e-09	0.15*	0.15	7.62	1.21	0.65
type 1-8	1248.46	495.59	0.16*	0.16	0.083	0.014	0.64

Table S7: Fit parameters for all damage functions for basic model type 2 and restricted to coastal counties. Same as **Table S5** but the affected population and per capita GDP is limited to the coastal counties affected by hurricane-power winds.

damage func.	α	$\Delta\alpha$	β_{Pop}	$\Delta\beta_{Pop}$	β_{GDPpc}	$\Delta\beta_{GDPpc}$	γ	$\Delta\gamma$	R^2
type 2-1	1.33e-13	2.87e-14	0.54	0.09	1.85	0.49	5.32	0.77	0.63
type 2-2	1.19e-05	5.42e-06	0.55	0.09	1.89	0.50	0.054	0.008	0.62
type 2-3	3.83e-14	9.19e-15	0.34	0.14	1.59	0.54	6.44	0.95	0.56
type 2-4	1.49e-04	9.56e-05	0.34	0.14	1.63	0.54	0.07	0.01	0.56
type 2-5	8.37e-21	2.39e-21	0.51	0.11	3.08	1.17	6.28	1.11	0.68
type 2-6	5.70e-12	2.68e-12	0.52	0.11	3.23	1.19	0.067	0.012	0.68
type 2-7	6.15e-21	1.66e-21	0.10*	0.14	2.74	1.10	7.71	1.15	0.69
type 2-8	2.56e-10	1.36e-10	0.10*	0.15	2.97	1.11	0.085	0.013	0.68

Table S8: Detailed overview of damage function types of basic model type 1 for ICAT only and time period 1980-2012. Same as **Table S2** but for ICAT only using the same time interval as NATCAT.

damage func.	socio-eco. scaling	loss data	# hurricanes	func. type	vmax-scaling	Pearson's r	AICc
type 1-1	GDP	icat-1980	52	global	power	0.84	102.6
type 1-2	GDP	icat-1980	52	global	exp	0.84	103.1
type 1-3	GDP	icat-1980	52	local	power	0.81	109.8
type 1-4	GDP	icat-1980	52	local	exp	0.81	109.9

Table S9: Detailed overview of damage function types of basic model type 2 for ICAT only and time period 1980-2012. Same as **Table S3** but for ICAT only using the same time interval as NATCAT.

damage func.	socio-eco. scaling	loss data	# hurricanes	func. type	vmax-scaling	Pearson's r	AICc
type 2-1	Pop/GDPpc	icat-1980	52	global	power	0.85	102.4
type 2-2	Pop/GDPpc	icat-1980	52	global	exp	0.85	102.6
type 2-3	Pop/GDPpc	icat-1980	52	local	power	0.83	109.1
type 2-4	Pop/GDPpc	icat-1980	52	local	exp	0.83	108.7

Table S10: Fit parameters for all damage functions of basic model type 1 for ICAT only and time period 1980-2012. Same as **Table S4** but for ICAT only using the same time interval as NATCAT. Values marked with a * differ non-significantly from zero.

damage func.	α	$\Delta\alpha$	β_{GDP}	$\Delta\beta_{GDP}$	γ	$\Delta\gamma$	R^2
type 1-1	3.45e-09	7.88e-10	0.64	0.09	5.52	1.04	0.68
type 1-2	0.74*	5.22	0.65	0.09	0.058	0.011	0.68
type 1-3	6.13e-10	1.71e-10	0.47	0.20	6.53	1.39	0.67
type 1-4	4.54*	10.81	0.48	0.20	0.070	0.015	0.67

Table S11: Fit parameters for all damage functions of basic model type 2 for ICAT only and time period 1980-2012. Same as **Table S5** but for ICAT only using the same time interval as NATCAT.

damage func.	α	$\Delta\alpha$	β_{Pop}	$\Delta\beta_{Pop}$	β_{GDPpc}	$\Delta\beta_{GDPpc}$	γ	$\Delta\gamma$	R^2
type 2-1	1.97e-18	6.16e-19	0.57	0.10	2.64	1.14	5.80	1.03	0.70
type 2-2	3.74e-10	2.03e-10	0.58	0.10	2.76	1.15	0.062	0.011	0.69
type 2-3	6.23e-20	1.95e-20	0.38	0.20	2.57	1.18	6.98	1.36	0.68
type 2-4	3.51e-10	2.00e-10	0.37	0.20	2.75	1.19	0.077	0.015	0.68

Figure S1: Wind-field for selected hurricanes. The wind-field for hurricane Betsy (**a**) is estimated using best-fit wind-radii based on the extended HURDAT2 track archive that contains wind-radii for all hurricanes since 1988 (c.f. **Table S1**). In contrast, the wind-field of hurricane Katrina (**b**) is reproduced using empiric wind-field data. The extension of 64 knts winds, that defines the affected region, and maximum winds, that determines the wind-speed at landfall, is clearly visible.

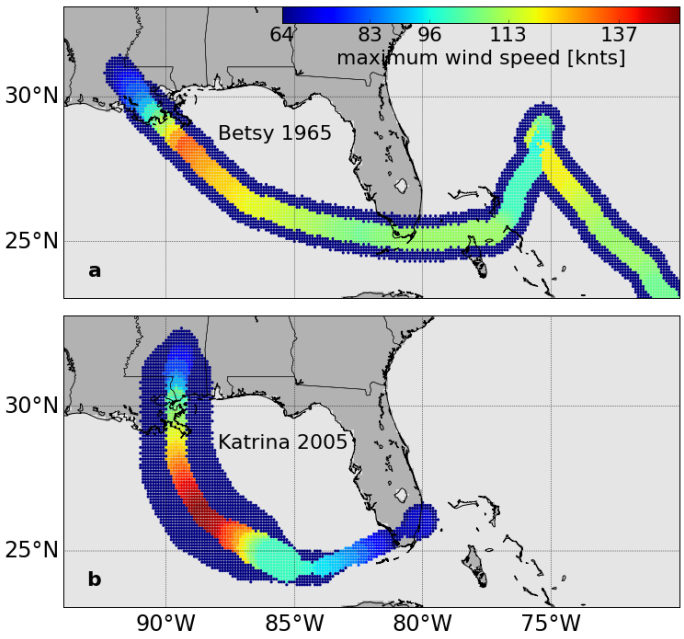

Figure S2: Overview of intensity normalization factors. For each GCM and each damage function of basic model type 1 (**a**) and type 2 (**b**) the factor is displayed by which the simulated median loss per hurricane between 1983-2012 exceeds the observed median loss. Intensity normalization is routinely done for all damage functions.

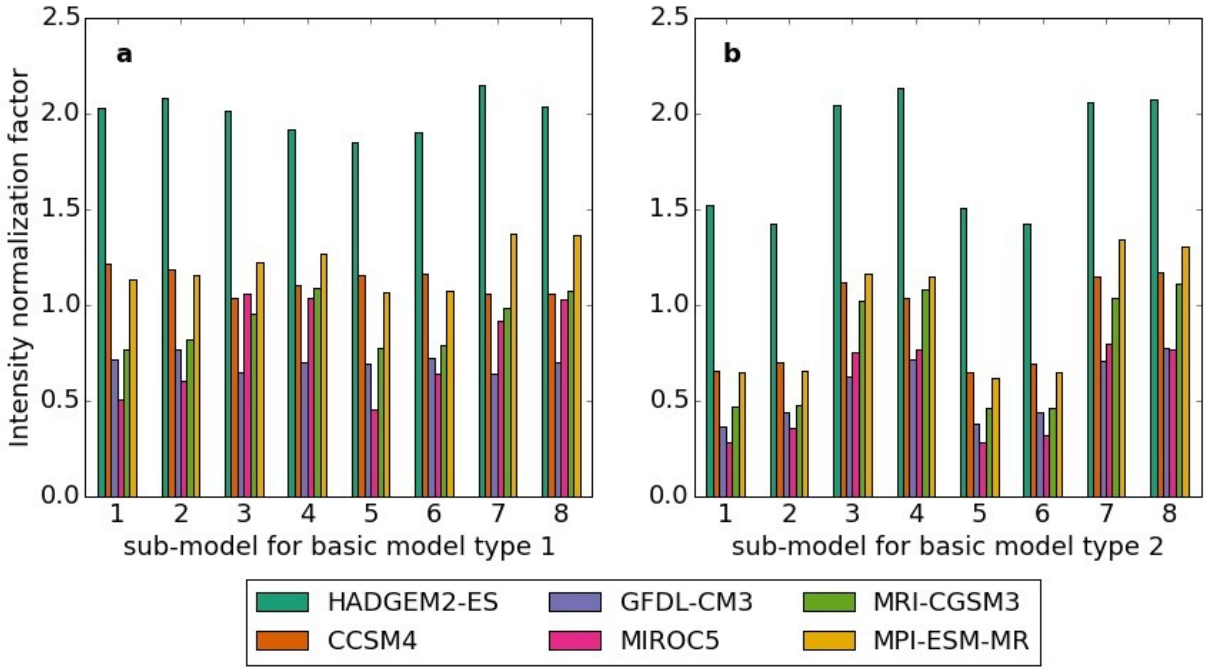

Figure S3: Overview of frequency normalization factors. For each GCM the factor is displayed by which the mean number of simulated hurricane landfalls (windspeed above 63knts) between 1993-2012 exceeds the mean number of observed landfalls. Frequency normalization is only required for annual loss projections.

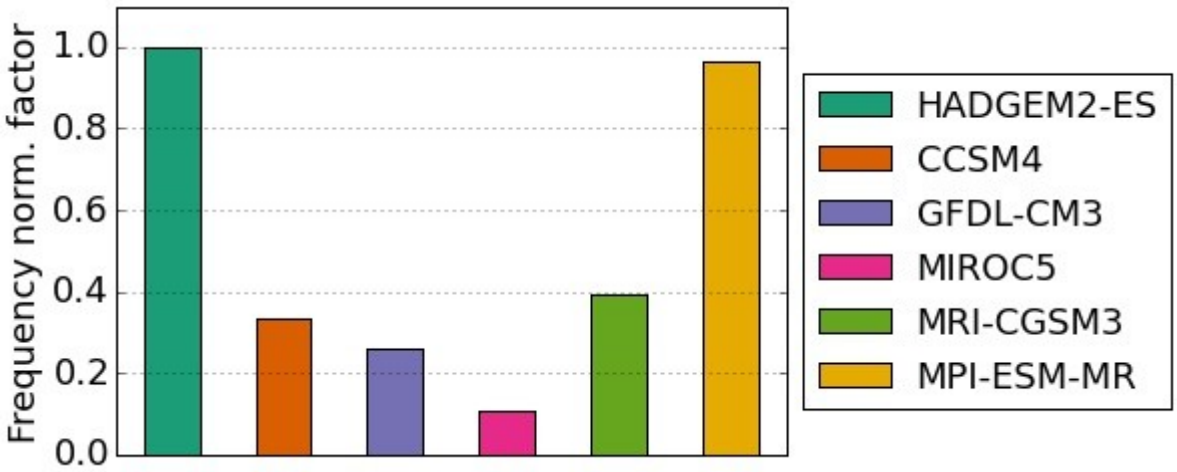

Figure S4: Non-linear scaling of historic hurricane losses with socio-economic development. The scaling of hurricane losses with each socio-economic parameter differs from a linear relationship with statistical significance (c.f. one-sided p-values in each panel). Negative (positive) slopes indicate sub- (super-) linear scaling of hurricane losses with (**a**) GDP, (**b**) GDP/capita, and (**c**) population. Lines are the best-fit through the empirical data based on 81 reported hurricanes from the ICAT archive. The **β**-values are the empirically obtained power-law exponents of the damage models of type 1 and type 2, described in the Methods section. Y-coordinates represent $\log_{10}\left[Loss_j/\left(\alpha \times exp\left(\gamma \times V_{max,j}\right)\right)\right] - \log_{10}\left(GDP_j\right)$ in panel a; $\log_{10}\left[Loss_j/\left(\alpha \times POP_j^{\beta_{Pop}} \times exp\left(\gamma \times V_{max,j}\right)\right)\right] - \log_{10}\left(GDPpc_j\right)$ in panel b; and $\log_{10}\left[Loss_j/\left(\alpha \times GDPpc_j{}^{\beta_{GDPpc}} \times exp\left(\gamma \times V_{max,j}\right)\right)\right] - \log_{10}\left(POP_j\right)$ in panel c.

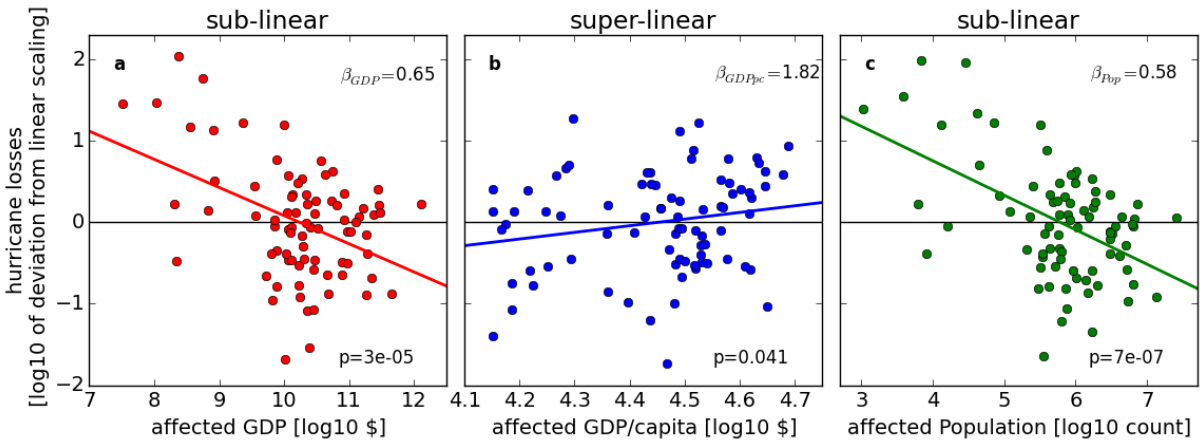

Figure S5: Non-linear scaling of historic hurricane losses with socio-economic development. Same as **Figure S4** but based on 53 reported hurricanes from the NATCAT archive and assuming a power-law relation between wind-speed and losses. Y-coordinates represent $\log_{10}\left[Loss_j/\left(\alpha \times {V_{max,j}}^{\gamma}\right)\right] - \log_{10}(GDP_j)$ in panel a; $\log_{10}\left[Loss_j/\left(\alpha \times POP_j^{\beta_{Pop}} \times {V_{max,j}}^{\gamma}\right)\right] - \log_{10}(GDPpc_j)$ in panel b; and $\log_{10}\left[Loss_j/\left(\alpha \times {GDPpc_j}^{\beta_{GDPpc}} \times {V_{max,j}}^{\gamma}\right)\right] - \log_{10}(POP_j)$ in panel c.

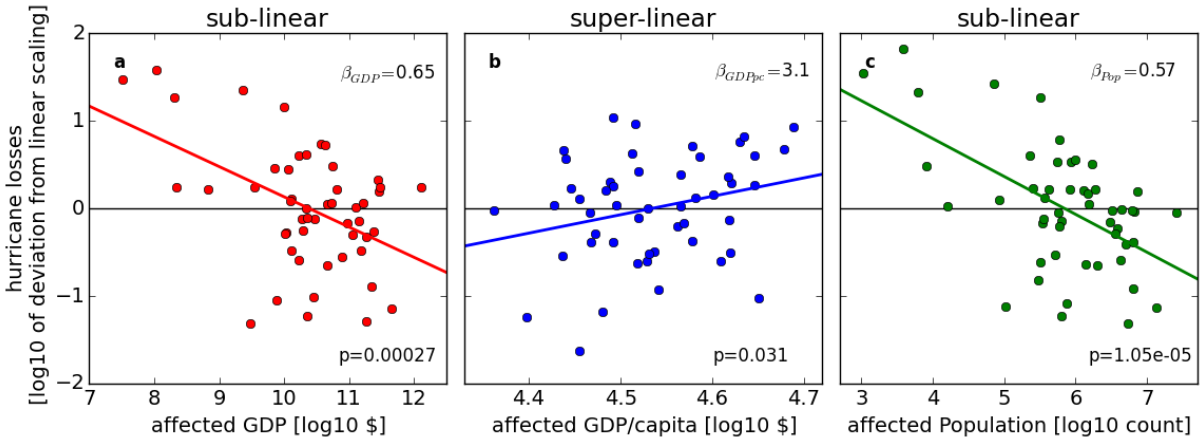

Figure S6: Non-linear scaling of historic hurricane losses with socio-economic development. Same as **Figure S4** but based on 53 reported hurricanes from the NATCAT archive and assuming an exponential relation between wind-speed and losses. Y-coordinates represent $\log_{10}\left[Loss_j/\left(\alpha \times exp\left(\gamma \times V_{max,j}\right)\right)\right] - \log_{10}\left(GDP_j\right)$ in panel a; $\log_{10}\left[Loss_j/\left(\alpha \times POP_j^{\beta_{Pop}} \times exp\left(\gamma \times V_{max,j}\right)\right)\right] - \log_{10}\left(GDPpc_j\right)$ in panel b; and $\log_{10}\left[Loss_j/\left(\alpha \times GDPpc_j^{\beta_{GDPpc}} \times exp\left(\gamma \times V_{max,j}\right)\right)\right] - \log_{10}\left(POP_j\right)$ in panel c.

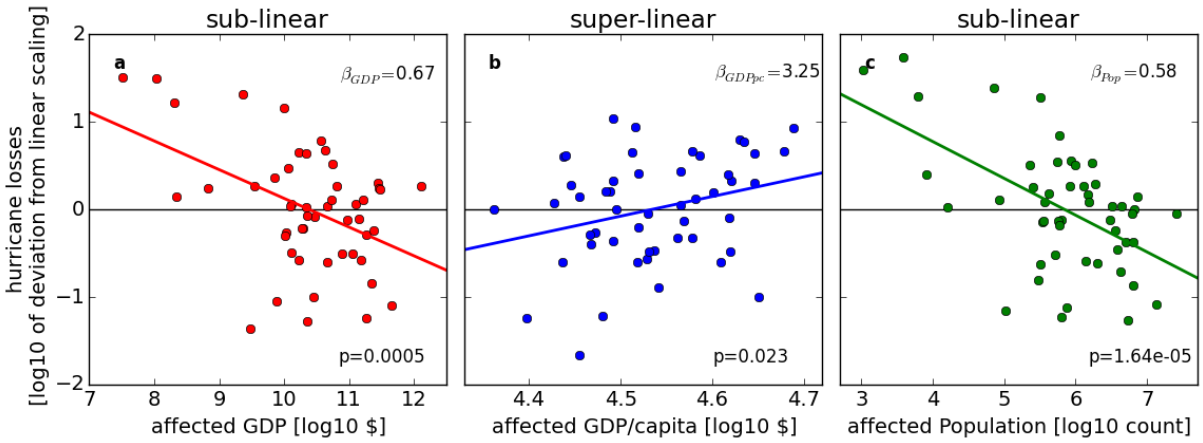

Figure S7: Amplification of relative future hurricane losses by rising per capita income. Projected average hurricane losses for 5 different future socio-economic development pathways (**a)**: SSP1, **b)**: SSP2, **c)**: SSP3, **d)**: SSP4, **e)**: SSP5) (blue line in each sub-figure) together with the separate contribution of GDP per capita and population change on projected losses. While population increase by itself (green line) leads to lower relative losses than projected with present-day socio-economic values (black line), growing GDP per capita (red line) results in substantially higher losses. Each data-point is the *decade-median* of all simulated hurricane losses based on 8 different damage projections and 6 GCMs. Loss/GDP (left axis) displays absolute losses according to the year's GDP while loss changes (right axis) are relative to corresponding 2010 values.

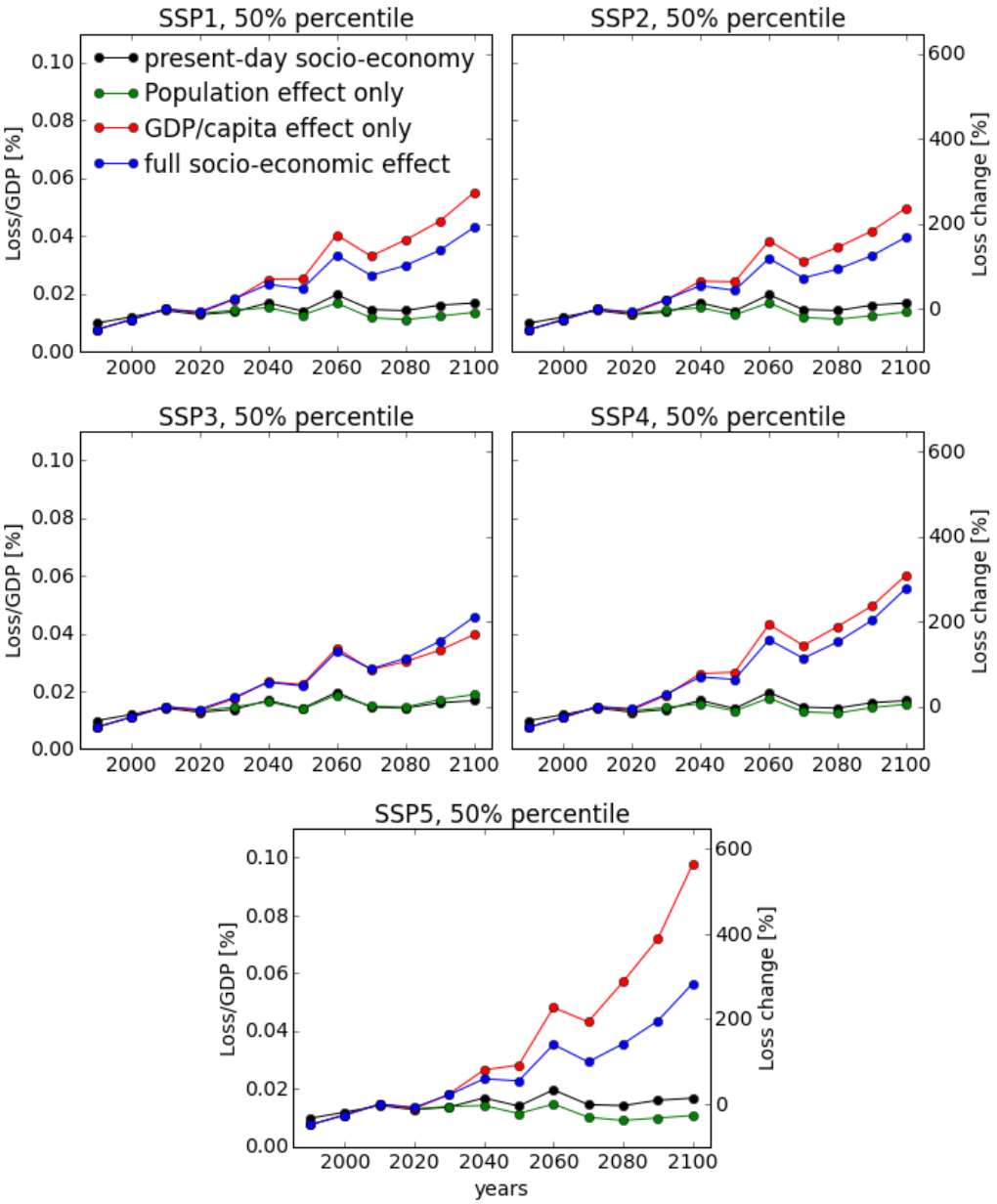

Figure S8: Amplification of relative future hurricane losses by rising per capita income. Same as **Figure S7** but now each data-point is the **95% percentile** of all simulated hurricane losses based on 8 different damage projections and the median of all 6 GCMs.

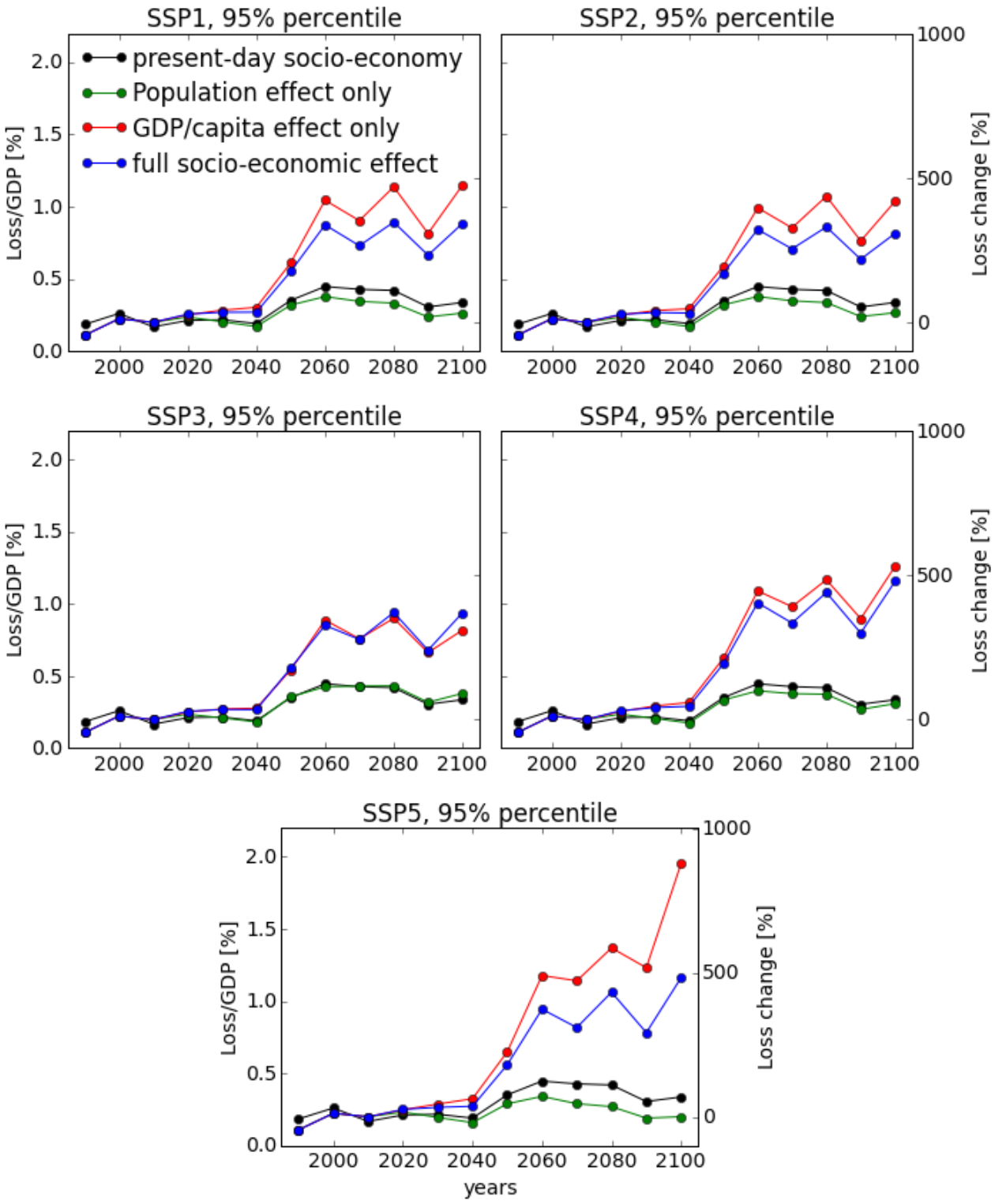

Figure S9: Impact of socio-economic predictors on future hurricane losses. Loss projections differ significantly whether the socio-economic predictors GDP per capita and population are treated separately (blue solid line, identical to Figure S7) or combined as total GDP (orange solid line). This difference is larger than the inter-model variability caused by the projections of individual damage models (dashed/dotted lines that span the shaded regions). Thick solid lines represent the decade-median over all GCMs and damage models. Dashed (dotted) lines are averages over both loss data sets only and correspond to damage models of global (local) functional form, see text and **Table S2** and **Table S3** for details.

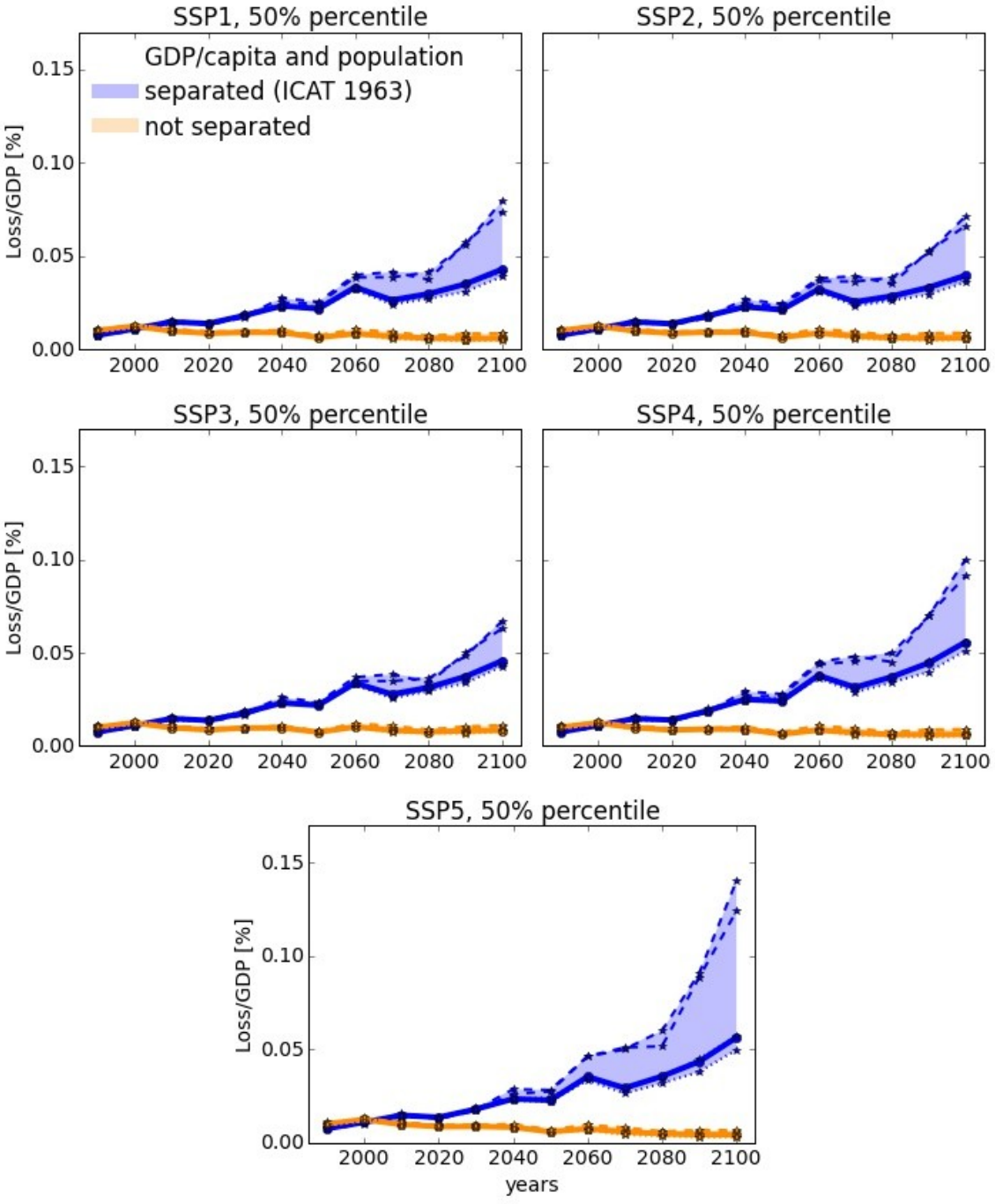

Figure S10: Impact of socio-economic predictors on future hurricane losses. Same as Figure S9 but the loss variability due to the separation of socio-economic predictors is now compared to the variability caused by different loss data. The spread caused by different loss data is large for separated socio-economic predictors (blue shaded plus hatched region) with NATCAT-driven models (dotted lines) higher than ICAT-driven models (dashed lines). This spread can be mainly contributed to the different time periods for which each loss data set is analyzed (ICAT 1963-2012, NATCAT 1980-2012). When both are analyzed from 1980-2012 (red-shaded area in Figure S10), the reduction in variability simultaneously results in an additional increase of average projected future losses (red solid line) compared to the increase presented in the main text (blue solid line).

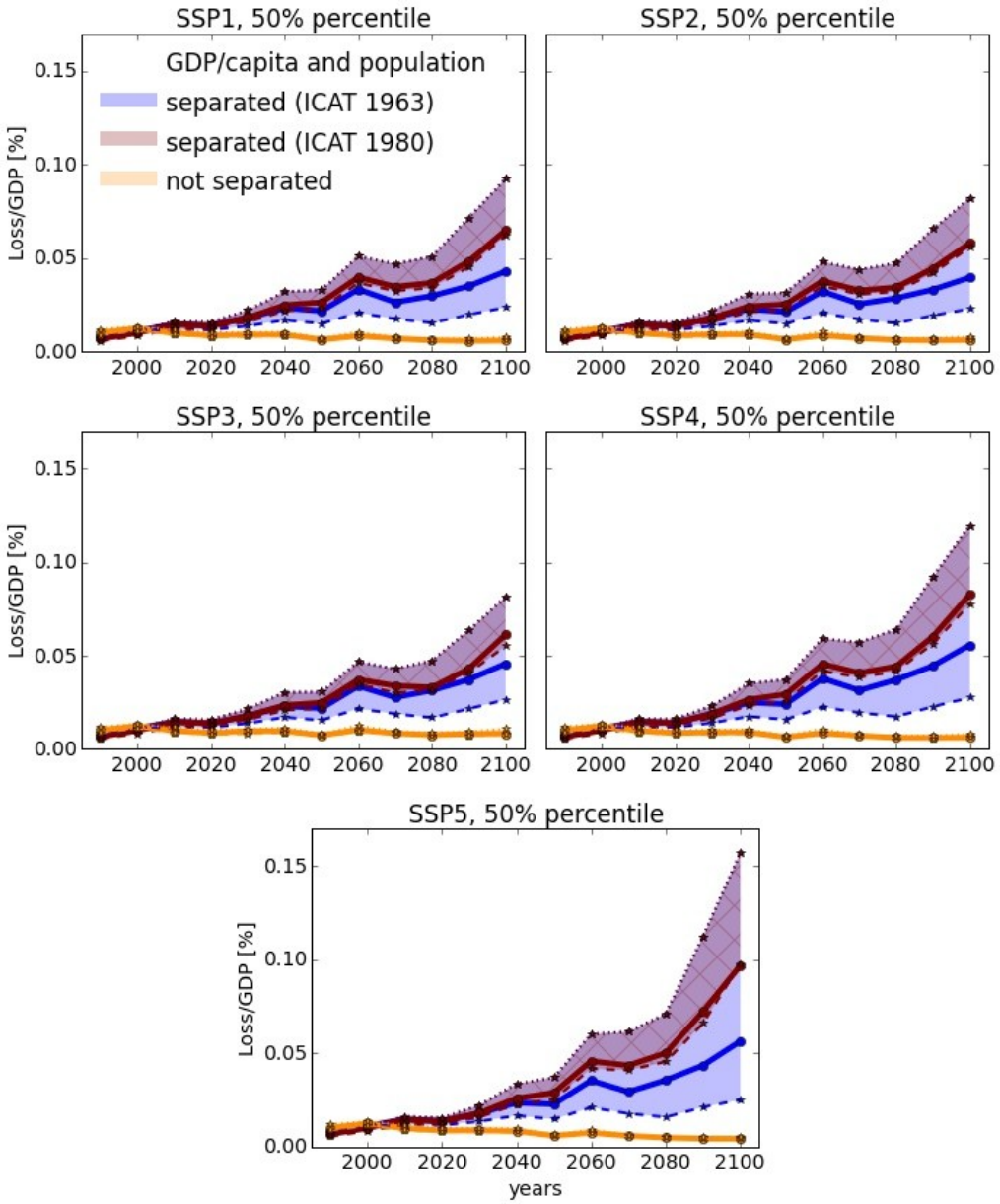

Figure S11: GCM-specific amplification of relative future hurricane losses by rising per capita income. Same as Figure S7 but future trends of average hurricane losses are analyzed separately for each GCM (**a,** MIROC5, **b,** GFDL-CM3, **c,** CCSM4, **d,** MRI-CGSM3, **e,** MPI-ESM-MR, **f,** HADGEM2-ES) and for SSP2 only. Loss changes are based on losses measured relative to national GDP and relative to 2010 values.

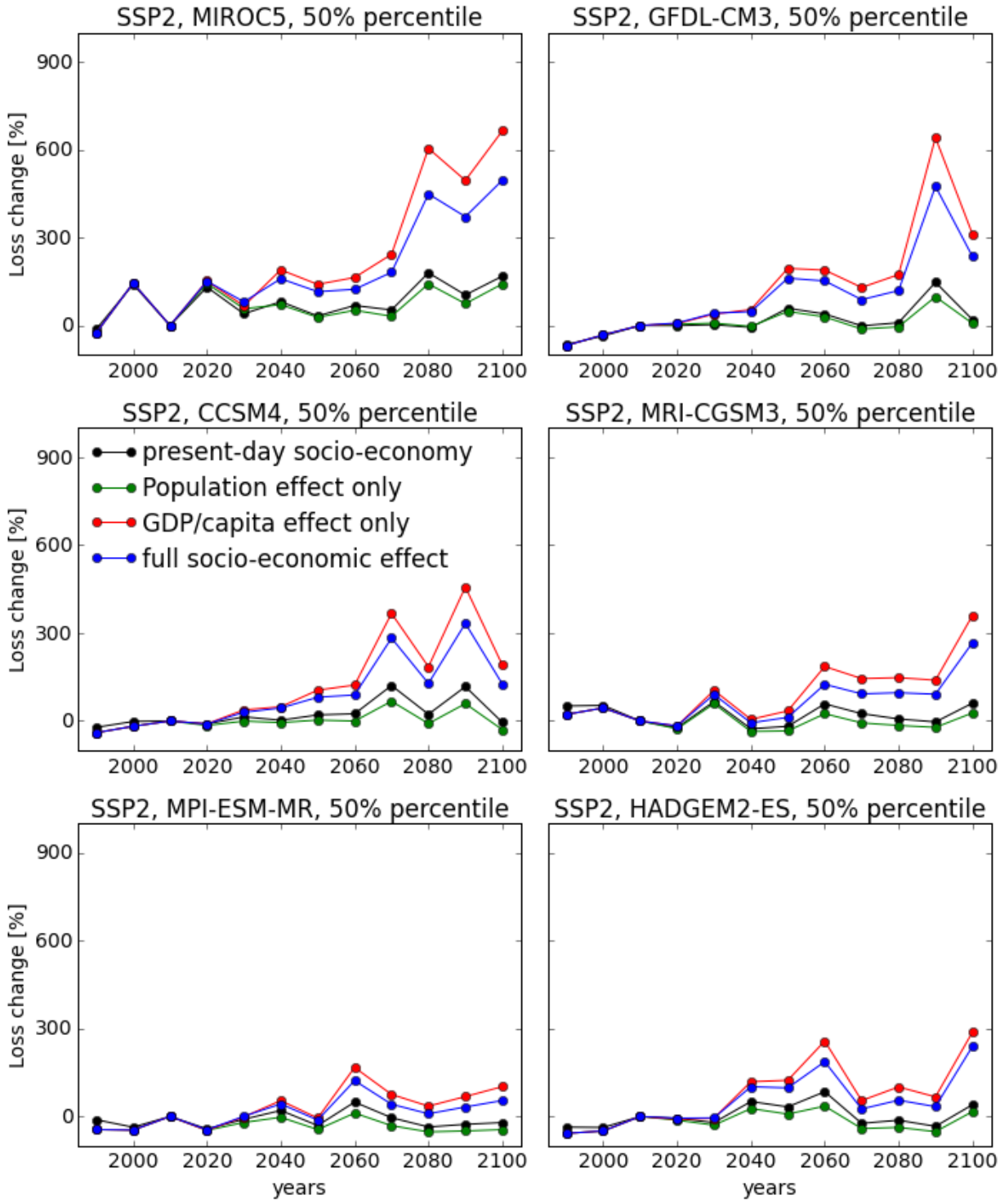

Figure S12: Amplification projected annual future hurricane losses by rising per capita income. Same as Figure S7 but here for annual losses, that aggregate changes in hurricane intensity and frequency. Each data-point is the decade-median of all simulated annual hurricane losses based on 8 different damage projections and 6 GCMs. Loss changes are based on losses measured relative to national GDP and relative to 2010 values.

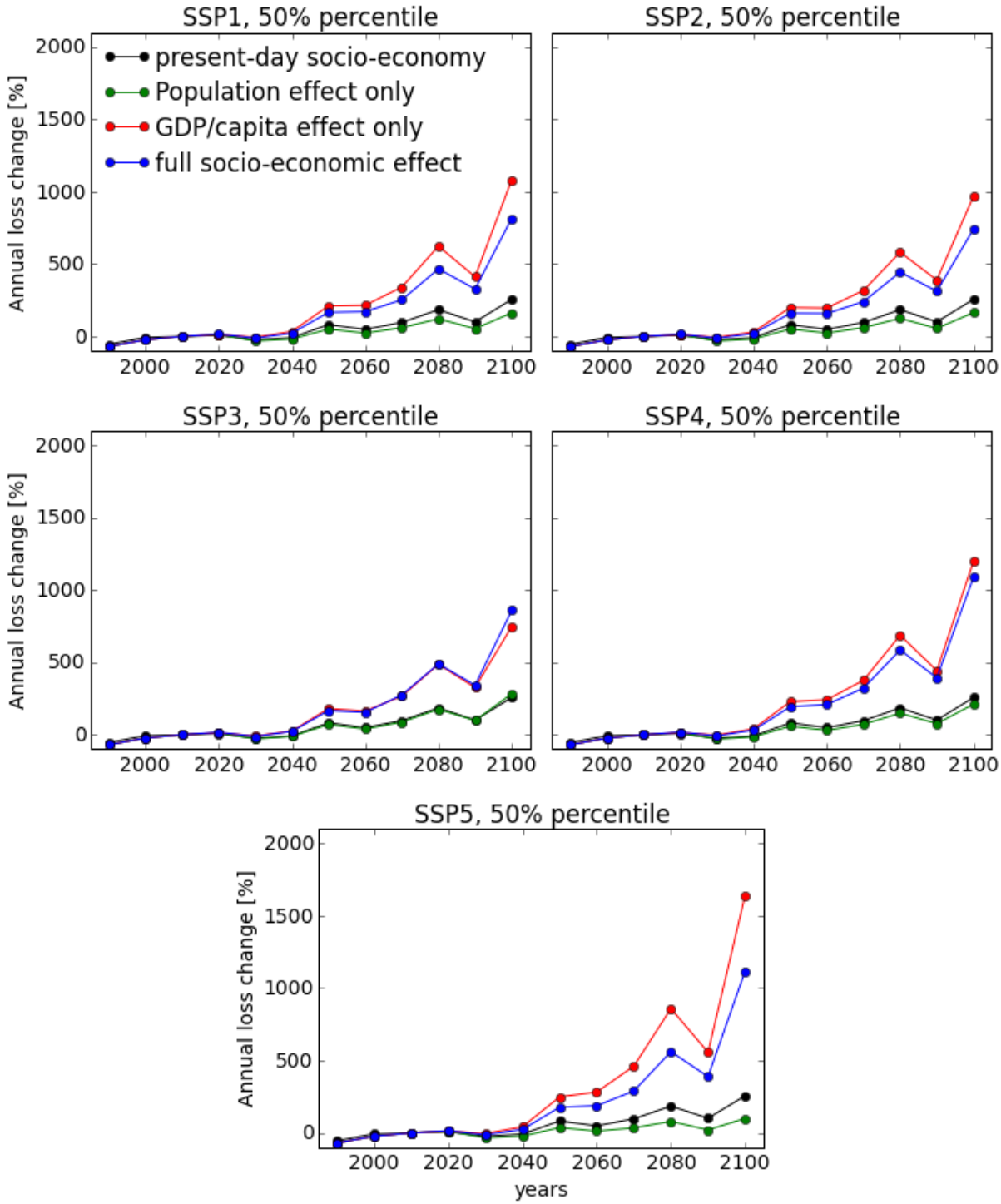

Supplementary References

1. Demuth, J. L., DeMaria, M. & Knaff, J. A. Improvement of advanced microwave sounding unit tropical cyclone intensity and size estimation algorithms. *J. Appl. Meteorol. Climatol.* **45,** 1573–1581 (2006).

2. Holland, G. A Revised Hurricane Pressure–Wind Model. *Mon. Weather Rev.* **136,** 3432–3445 (2008).

3. Emanuel, K. Downscaling CMIP5 climate models shows increased tropical cyclone activity over the 21st century. *Proc. Natl. Acad. Sci. U. S. A.* **110,** 12219–24 (2013).

4. Pielke, R. A. *et al.* Normalized Hurricane Damage in the United States: 1900–2005. *Nat. Hazards Rev.* **9,** 29–42 (2008).

5. Kron, W., Steuer, M., Löw, P. & Wirtz, A. How to deal properly with a natural catastrophe database - Analysis of flood losses. *Nat. Hazards Earth Syst. Sci.* **12,** 535–550 (2012).

6. Jongman, B., Ward, P. J. & Aerts, J. C. J. H. Global exposure to river and coastal flooding: Long term trends and changes. *Glob. Environ. Chang.* **22,** 823–835 (2012).

7. Hallegatte, S., Green, C., Nicholls, R. J. & Corfee-Morlot, J. Future flood losses in major coastal cities. *Nat. Clim. Chang.* **3,** 802–806 (2013).

8. *Gridded Population of the World, Version 3 (GPWv3)*. *Cent. Int. Earth Sci. Inf. Netw. (CIESIN), Cent. Int. Agric. Trop. (CIAT),* (CIESIN, Columbia University, 2005).

9. Minnesota Population Center. *National Historical Geographic Information System: Version 2.0*. (University of Minnesota, 2011).

10. B. Jones and B. O'Neill. Spatially explicit global population scenarios for the shared socioeconomic pathways. *Environ. Res. Lett.* **submitted,** (2015).

11. Emanuel, K. Global Warming Effects on U.S. Hurricane Damage. *Weather. Clim. Soc.* **3,** 261–268 (2011).

12. Nordhaus, W. D. The Economics of Hurricanes and Implications of Global Warming. *Clim. Chang. Econ.* **01,** 1–20 (2010).

13. Bedrick, E. J. & Tsai, C.-L. Model Selection for Multivariate Regression in Small Samples. *Biometrics* **50,** 226 (1994).

14. Holland, G. & Bruyère, C. L. Recent intense hurricane response to global climate change. *Clim. Dyn.* **42,** 617–627 (2014).

15. Knutson, T. R. *et al.* Global Projections of Intense Tropical Cyclone Activity for the Late Twenty-First Century from Dynamical Downscaling of CMIP5/RCP4.5 Scenarios. *J. Clim.* 150729114230005 (2015).

16. Knutson, T. R. *et al.* Tropical cyclones and climate change. *Nat. Geosci.* **3,** 157–163 (2010).

17. Villarini, G. & Vecchi, G. A. Twenty-first-century projections of North Atlantic tropical storms from CMIP5 models. *Nat. Clim. Chang.* **2,** 604–607 (2012).

18. Walsh, K. J. E. *et al.* Hurricanes and Climate: The U.S. CLIVAR Working Group on Hurricanes. *Bull. Am. Meteorol. Soc.* **96,** 997–1017 (2015).

19. Reed, A. J., Mann, M. E., Emanuel, K. A. & Titley, D. W. An analysis of long-term relationships among count statistics and metrics of synthetic tropical cyclones downscaled from CMIP5 models. *J. Geophys. Res. Atmos.* **120,** 7506–7519 (2015).

20. Emanuel, K., Sundararajan, R. & Williams, J. Hurricanes and Global Warming: Results from Downscaling IPCC AR4 Simulations. *Bull. Am. Meteorol. Soc.* **89,** 347–367 (2008).